JOURNAL OF NATURAL PRODUCTS

Article

pubs.acs.org/jnp

Isolation, Characterization, and Synthesis of the Barrettides: Disulfide-Containing Peptides from the Marine Sponge *Geodia barretti*

Bodil B. Carstens,[†] K. Johan Rosengren,[‡] Sunithi Gunasekera,[§] Stefanie Schempp,[§] Lars Bohlin,[§] Mia Dahlström,[⊥] Richard J. Clark,[‡] and Ulf Göransson*[,§]

[†]Institute for Molecular Bioscience and [‡]School of Biomedical Sciences, University of Queensland, Brisbane, QLD 4072, Australia

[§]Division of Pharmacognosy, Department of Medicinal Chemistry, Biomedical Center, Uppsala University, Box 574, SE-751 23 Uppsala, Sweden

[⊥]Department of Chemistry, Materials and Surfaces, SP Technical Research Institute of Sweden, Arvid Wallgrens Backe 20, SE-413 46 Göteborg, Sweden

Supporting Information

ABSTRACT: Two disulfide-containing peptides, barrettides A (**1**) and B (**2**), from the cold-water marine sponge *Geodia barretti* are described. Those 31 amino acid residue long peptides were sequenced using mass spectrometry methods and structurally characterized using NMR spectroscopy. The structure of **1** was confirmed by total synthesis using the solid-phase peptide synthesis approach that was developed. The two peptides were found to differ only at a single position in their sequence. The three-dimensional structure of **1** revealed that these peptides possess a unique fold consisting of a long β-hairpin structure that is cross-braced by two disulfide bonds in a ladder-like arrangement. The peptides are amphipathic in nature with the hydrophobic and charged residues clustered on separate faces of the molecule. The barrettides were found not to inhibit the growth of either *Escherichia coli* or *Staphylococcus aureus* but displayed antifouling activity against barnacle larvae (*Balanus improvisus*) without lethal effects in the concentrations tested.

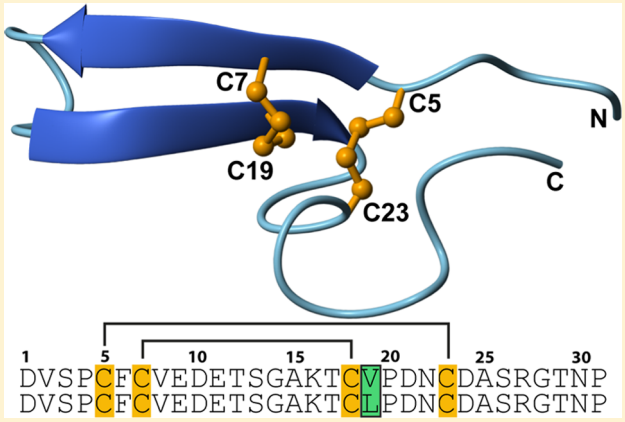

Disulfide-rich peptides from marine sources such as the conotoxins from snails of the *Conus* genus and the cnidarian peptide toxins are a diverse source of biologically active molecules for use as both drug leads and pharmacological tools.[1−6] These disulfide-containing peptides typically range from 1.5 to 5 kDa in molecular weight and contain multiple cysteines forming a network of disulfide bonds that stabilize the peptide and define its three-dimensional structure. For example, the conotoxins exhibit vast variations in the number, spacing, and connectivity of cysteines, resulting in 26 cysteine frameworks (defined by the number and spacing of the cysteine residues) and 12 different classes of folds (defined by the cystine framework and the disulfide pattern).[7,8] Disulfide-rich peptides interact with a range of molecular targets including ion channels, membrane transporters, and receptors with exquisite potency and selectivity for their molecular target.[4,9] One reason for the potency and selectivity of these peptides is that the disulfide bonds provide a stable framework on which specific residues within the intercysteine loops can be incorporated to maximize the interaction with the molecular target.

Marine sponges have been a rich source of a range of bioactive natural products including both organic molecules and peptides.[10,11] Interestingly, despite the diverse range of disulfide-rich peptides from other phyla and classes of marine organisms, there have been very few disulfide-rich peptides described from marine sponges. The bacterial sialidase inhibitor asteropine A was the first disulfide-rich peptide to be described from a marine sponge, *Asteropsus simplex* Carter.[12] Asteropine A contains 36 amino acids with six cysteines that form three disulfide bonds in a knotted topology. This cystine knot is a common motif in disulfide-rich peptides, including conotoxins, presumably because it imparts substantial stability to the molecule.[13] Another type of cystine-knot peptide, the asteropsins, from an *Asteropsus* species has also recently been described. The asteropsins have the same cystine framework as asteropine A, but there is little conservation within the remainder of the sequence. This is also a common feature seen in other disulfide-rich peptides such as conotoxins, spider toxins, and the plant-derived cyclotides, where a conserved

Received: March 8, 2015
Published: July 29, 2015

DOI: 10.1021/acs.jnatprod.5b00210
J. Nat. Prod. 2015, 78, 1886−1893

disulfide framework is used as a template to generate a "combinatorial library" of peptides, even within the same species.[9,14,15] The neopetrosiamides, isolated from a *Neopetrosia* sp. sponge, like asteropine A and the asteropsins also contain six cysteines, but they form an alternate disulfide arrangement, CysI-V, CysII-IV, and CysIII-VI.[16] These peptides are potent inhibitors of amoeboid invasion by human tumor cells[17] via the disruption of cell adhesion through loss of cell surface integrins.[18] Chemical synthesis of neopetrosiamide A using solid-phase peptide synthesis (SPPS) methods and an orthogonal cysteine protection strategy was subsequently used to determine the disulfide connectivity of the peptide.[16] Being able to produce neopetrosiamide A synthetically has also facilitated structure/activity studies, which revealed the key role that the disulfide bonds play in defining the bioactive conformation of neopetrosamide A, as alternate disulfide isomers of this peptide were biologically inactive.[19]

The marine sponge *Geodia barretti* Bowerbank (family Geodiidae, order Tetractinellida, class Demospongiae), a cold-water marine sponge found on the north Atlantic continental shelf, has been found to produce a wide range of secondary metabolites including several cyclic dipeptides derived from tryptophan and arginine, known as the barettins.[20−22] The barettins have recently been shown to act in synergy to deter larvae of surface settlers,[23] and field trials using barettins incorporated into paint were shown to prevent surface fouling by barnacles (*Balanus improvisus*) and blue mussels (*Mytilis edulis*).[24] More recently, barettin was shown to be an antioxidant and also inhibited secretion of several pro-inflammatory cytokines from LPS-stimulated THP-1 cells.[25]

In this study we describe the isolation and characterization of two novel disulfide-containing peptides from *G. barretti*, which we have named barrettides A (**1**) and B (**2**). We further characterized **1** by determining its three-dimensional structure using NMR spectroscopy and also developed an efficient approach to chemically synthesize these peptides, which can be used for future structure/activity studies. Finally, we describe the antibacterial and antifouling properties of both **1** and **2**.

RESULTS AND DISCUSSION

A specimen of the cold-water marine sponge *G. barretti*, obtained from the Swedish Kosterfjord, was extracted with CH_3CN/H_2O, and compounds were purified extensively by RP-HPLC and size-exclusion chromatography, as shown in Figure 1. Mass spectrometry analysis of the extract revealed two major peaks corresponding to two peptides present in all three extraction steps, termed barrettides A (**1**) and B (**2**). Mass ions 1607.4 and 1072.2 correspond to $[M + 2H]^{2+}$ and $[M + 3H]^{3+}$, respectively, for **1**, and mass ions 1614.4 and 1076.6 correspond to $[M + 2H]^{2+}$ and $[M + 3H]^{3+}$, respectively, for **2**. After RP-HPLC (first purification step) and size-exclusion chromatography (second purification step) the recovered yield of the peptides was 2.3% from the extract. The recovered yield for purified peptides based on RP-HPLC recovery (third purification step) was 2.2% and 1.0% (from the extract) for **1** and **2**, respectively. In total, four novel peptides with $[M + 2H]^{2+}$ ions of 1607 (**1**), 1614 (**2**), 1619, and 1648 were extracted and isolated. The latter two were present in small quantities, so further studies focused on barrettides A and B. The monoisotopic masses (M) for **1** and **2** were determined to be 3212.3862 and 3226.4175, respectively, by deconvolution of their $[M + 3H]^{3+}$ ions.

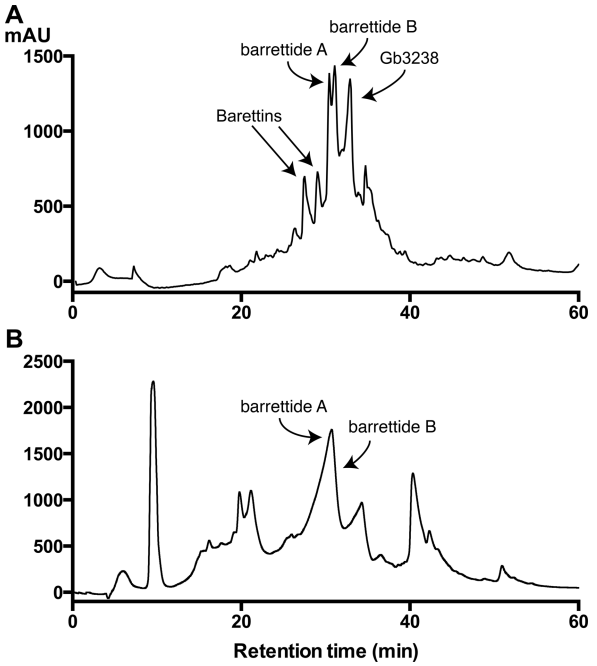

Figure 1. RP-HPLC traces of the isolation and separation of peptides from an extract of *G. barretti*. (A) The previously described barettins eluted after ∼28 min, whereas the two novel peptides barrettides A (**1**) and B (**2**) eluted after ∼30 min. The peptide displaying a $[M + 2H]^{2+}$ ion of 1619 termed Gb3238 eluted after ∼32 min. The peptide with an $[M + 2H]^{2+}$ ion of 1648 was not detected in these initial isolation studies. RP-HPLC purification was performed on a 1.5% buffer B/min gradient, and absorbance was measured at 215 nm. (B) RP-HPLC trace after size exclusion chromatography showing the peak comprising **1** and **2** eluting after 30 min. RP-HPLC purification was performed on a 0.5% buffer B/min gradient starting at 25% buffer B. Absorbance was measured at 215 nm.

The amino acid content of **1** and **2** was quantitatively determined after 24 h hydrolysis with 6 M HCl to assist the sequencing and indicated the presence of six Asp/Asn, three Thr, three Ser, three Pro, three Val, two Glu/Gln, two Gly, two Ala, one Phe, one Lys, and one Arg residue for **1**. Amino acid analysis of **2** revealed it contained the same amino acid content as **1** except there were only two Val residues and an additional Leu residue. Furthermore, peptides were treated with dithiothreitol (DTT) to break disulfide bonds and subsequently alkylated using iodoacetamide (IAM) to block reactive cysteine residues. Following reduction and alkylation, an increase in 232 Da was observed for both peptides, corresponding to alkylation of four cysteines involved in two disulfide bonds. Hence, the monoisotopic masses can then be calculated to be 3212.2791 and 3226.2948 Da for **1** and **2**, which corresponds to deviations of 33 and 38 ppm, respectively, from their experimentally determined masses. In our hands, this is within the normal range of the instrument used (a Waters Qtof Micro) considering the size of the molecules.

The reduced and alkylated peptides were cleaved with various enzymes, including trypsin, chymotrypsin, and endoproteinase Glu-C, in order to elucidate their sequences. These cleavage mixtures were analyzed using LC-MS-MS for sequence determinations. The major fragments and their sequence sections for both peptides are shown in Figure 2. Fragments discovered from trypsin digestion revealed major fragments with monoisotopic masses of 1800.4 Da for both peptides, which were sequenced to be DVSPCFCV-

DOI: 10.1021/acs.jnatprod.5b00210
J. Nat. Prod. 2015, 78, 1886−1893

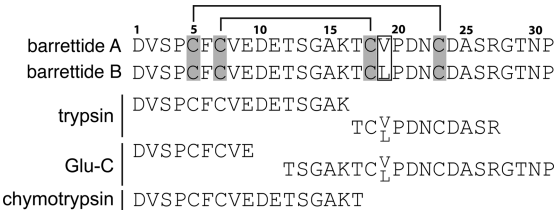

Figure 2. Sequences of peptides isolated from the cold-water sponge *G. barretti*. The sequences of barrettides A (**1**) and B (**2**) were determined using MS/MS sequencing of peptide fragments from enzymatic digests in combination with amino acid analysis. Sequence fragments identified from the trypsin, Endo-GluC, and chymotrypsin digests are shown. Barrettides A and B differ only at position 19, where **1** has a Val, whereas **2** has a Leu. Both peptides have four Cys residues that form two disulfide bonds between residues Cys5−Cys23 and Cys7−Cys18. Cys residues are highlighted in gray, and the sequence difference at position 19 between the two peptides is highlighted by a box.

EDETSGAK. Additionally, two fragments with monoisotopic masses of 1294.5 and 1308.5 Da were sequenced to be TCVPDNCDASR and TCLPDNCDASR for **1** and **2**, respectively. Additional fragments from Glu-C digestion were sequenced to be DVSPCFCVEDE for both peptides and TSGAKTCVPDNCDASRGTNP for **1** and TSGAKTCLPDN-CDASRGTNP for **2**. Moreover, chymotrypsin digestion resulted in a fragment with a monoisotopic mass of 1901.4, which was sequenced to be DVSPCFCVEDETSGAKT for both peptides. Chymotrypsin cleavage data also helped in determining the order of the last four residues at the C-terminus of each peptide to be GTNP.

These sequence fragments in combination with the amino acid quantification data yielded the complete sequences of the two peptides to be determined as DVSPCFCVED-ETSGAKTCVPDNCDASRGTNP and DVSPCFCVED-ETSGAKTCLPDNCDASRGTNP for **1** and **2**, respectively, as shown in Figure 2. NMR spectroscopy was also used to confirm the sequences. The sole difference between the sequences of the two peptides is at position 19, where **1** has a valine, whereas **2** has a leucine residue. A search to identify peptides related to the barrettides using both tBLASTN and BLASTp[26] revealed no other identical or similar peptide sequences in the NCBI databases. A recent study[27] reported the metatranscriptome (complete set of gene transcripts) of *G. barretti*. Using Ugene,[28] the peptide sequences of **1** and **2** were matched against the *G. barretti* transcriptome. Surprisingly, only one hit, DVSPCFCVEDETSGAKTCVPDLSGLAR, shared similar sequence sections to the novel peptides found in this study, which was reported to be 82% and 78% for **1** and **2**, respectively. Its monoisotopic mass does not match one of the low-abundant peptides that was isolated from the sponge. The hit matches **1** from Asp1−Asp21, but differs in the C-terminal region including missing the fourth cysteine, which is required if two disulfide bonds are to be formed. It is possible that differences in time and location of specimen collection between the sponge sample used in this study and the specimen of *G. barretti* used for the metatranscriptomics study, which was collected off the Norwegian west coast,[27] could explain the discrepancy between our study and the transcriptomic data. In addition to that possibility of variation of gene expression, it cannot be ruled out that this particular sequence escaped sequencing.

NMR data were recorded at 298 K for extracted and purified **1** and **2**. Homonuclear spectra were assigned using the sequential assignment procedure.[29] Briefly TOCSY and DQF-COSY data were used to identify individual spin systems, and NOESY data were used to link neighboring residues in the sequence. The fingerprint region of the NOESY spectrum is shown in Supplementary Figure 1. Sequential αH_i-NH_{i+1} NOEs were observed for the entire peptide chains, except at Pro4, Pro20, and Pro31, because these residues lack amide protons. Pro4 and Pro31 were found to be in a *trans* configuration, as indicated by intense Hα−Hδ NOEs between the preceding residue and the Pro, whereas Pro20 was in a *cis* configuration, as indicated by intense Hα−Hα NOEs between residue 19 and Pro20. The NMR spectra recorded showed single spin systems for each residue, except for residues 29−31, where a second minor conformation was apparent due to *cis*−*trans* isomerization of Pro31.

Secondary Hα NMR chemical shifts are the difference between the observed chemical shift and the corresponding random coil value and are strong indicators of the presence of secondary structure in peptides.[30] Analysis of the measured chemical shifts for both peptides revealed two series of positive secondary Hα shifts between residues 6−9 and 16−19, as shown in Figure 3, which is indicative of β-sheet regions. The

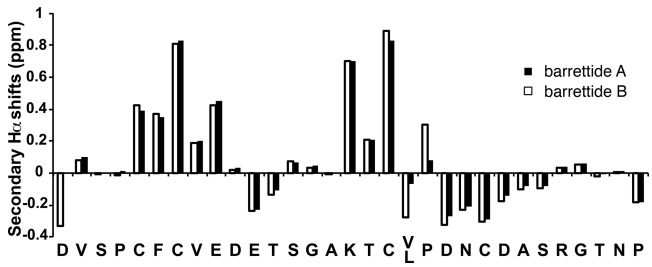

Figure 3. Secondary Hα chemical shifts for barrettides A (**1**) and B (**2**). Their sequences are indicated at the bottom of the figure, aligned with their corresponding point in the traces. Barrettide A (**1**) is represented in black bars, whereas Barrettide B (**2**) is represented in white bars. The trend in secondary Hα shifts is identical, indicating that their secondary structures will be very similar, although there are some clear differences at positions 19 and 20, due to the different amino acids at position 19, where **1** has a Val and **2** has a Leu.

NH of Asp1 of **2** could not be observed, as the free amine of the N-terminal residue is rapidly exchanging with the solvent. However, Asp1 Hα and Hβ protons of **1** could be located in the $^{1}H-^{13}C$ HSQC spectrum of this peptide. The NMR secondary shift values for **1** and **2** follow the same pattern with some small localized variations at positions 19−20 due to the nature of the different amino acids at position 19. Overall, this indicates that they have identical three-dimensional structures and perhaps similar bioactivities.

The NMR spectroscopy data were used to determine the three-dimensional structure of **1**. Structural restraints (Table 1) included interproton distances generated from NOE intensities, and backbone dihedral angle restraints (ψ and φ angles) were obtained from the angles predicted by TALOS-N analysis using the HN, Hα, N, Cα, and Cβ chemical shifts.[31,32] The χ^1 dihedral angle conformations and stereospecific assignments of Hβ methylene pairs were determined from intraresidue NOE patterns derived from a 100 ms NOESY spectrum together with $^{3}J_{H\alpha-H\beta}$ coupling patterns from the DQF-COSY spectrum. Cys7 and Cys18 were found to have χ^1 dihedral angles of −60°,

DOI: 10.1021/acs.jnatprod.5b00210
J. Nat. Prod. 2015, 78, 1886−1893

Table 1. Energies and Structural Statistics for the Family of the 20 Lowest Energy Structures with Highest MolProbity Scores for Barrettide A (1)

Energies (kcal/mol)	
overall	−964.7 ± 13.26
bonds	14.31 ± 0.281
angles	38.21 ± 1.00
improper	15.45 ± 0.729
van der Waals	−73.21 ± 1.59
NOE	0.084 ± 0.004
cDih	0.275 ± 0.055
dihedral	133.7 ± 0.25
electrostatic	−1093.0 ± 13.4
MolProbity Statistics	
clashes (0.4 Å/1000 atoms)	7.248 ± 0.6556
poor rotamers	0.185 ± 0.185
Ramachandran outliers	1.035 ± 0.440
Ramachandran favored	94.14 ± 0.97
MolProbity score[a]	1.728 ± 0.0497
MolProbity score percentile[b]	86.90 ± 1.73
residues with bad bonds	0.00 ± 0.00
residues with bad angles	0.00 ± 0.00
Atomic rmsd[c]	
mean global backbone	0.92 ± 0.34 Å
mean global heavy	1.58 ± 0.35 Å
Distance Restraints	
intraresidue ($i - j = 0$)	67
sequential ($\|i - j\| = 1$)	107
medium range ($1 < \|i - j\| < 5$)	39
long range ($\|i - j\| \geq 5$)	60
hydrogen bonds	16 (for 8 H-bonds)
total	289
Dihedral Angle Restraints	
ϕ	18
χ^1	10
total	28
Violations from Experimental Restraints	
total NOE violations exceeding 0.2 Å	1 (0.226 Å)
total dihedral violations exceeding 3.0°	0

[a]MolProbity score combines the Clashscore, rotamer, and Ramachandran evaluations into a single score, normalized to be on the same scale as X-ray resolution. [b]100th percentile is the best among structures of comparable resolutions; 0th percentile is the worst. [c]Atomic rmsd values are for residues 5−23.

Cys5, Asp10, and Asp21 have χ^1 dihedral angles of 180°, and Cys23 has a χ^1 dihedral angle of +60°. Additionally, another four χ^1 angles were incorporated into the structure calculations based on the TALOS-N analysis. Amide protons involved in hydrogen-bonding interactions were identified by deuterium exchange experiments and temperature coefficient data. The slow exchange of the amide protons of Val8, Thr17, and Val19 with deuterated water suggested that these three residues were involved in hydrogen bonding. Moreover, amide protons with temperature coefficients > −4.6 ppb/K are considered as being protected from the solvent and are thus probably engaged in hydrogen bonds.[33] The amide protons of residues Phe6, Val8, Thr12, Gly14, Ala15, Thr17, Val19, and Cys23 exhibited temperature insensitivity indicative of hydrogen-bonding involvement. In total, 16 restraints for eight hydrogen bonds were included in the NMR structure determination based on analysis of slow exchanging amides and temperature coefficient data. These eight hydrogen bonds were identified as follows based on structure calculations: Phe6−Val19 O, Val8−Thr17 O, Thr12−Asp10 OD1/2, Gly14−Asp10 O, Ala15−Asp10 O, Thr17−Val8 O, Val19−Phe6 O, and Cys23−Pro20 O. NMR analysis revealed strong NOE cross-peaks between Cys5 and Cys23 and between Cys7 and Cys18, suggesting the disulfide connectivity to be 5−23 and 7−18. The Cys7−Cys18 disulfide bond is situated between two strands in a β-sheet, and a strong Hα−Hα peak was observed between them. To further confirm the disulfide connectivity, a set of structures with the two other possible disulfide connectivities was calculated. The resulting higher energies and more restraint violations from the calculated structures with the two other possible disulfide connectivities, i.e., Cys5−Cys18 and Cys7−Cys23, and Cys5−Cys7 and Cys18−Cys23, showed that the Cys5−Cys23 and Cys7−Cys18 connectivity was structurally favorable, which was further supported by the consistency between experimentally determined χ^1 dihedral angles and the conformation of the disulfide bonds.

A set of 50 structures was calculated, and the best 20 structures based on lowest overall energies and good covalent geometries judged by MolProbity scores were chosen to represent the solution structure of **1** (Figure 4). Structural

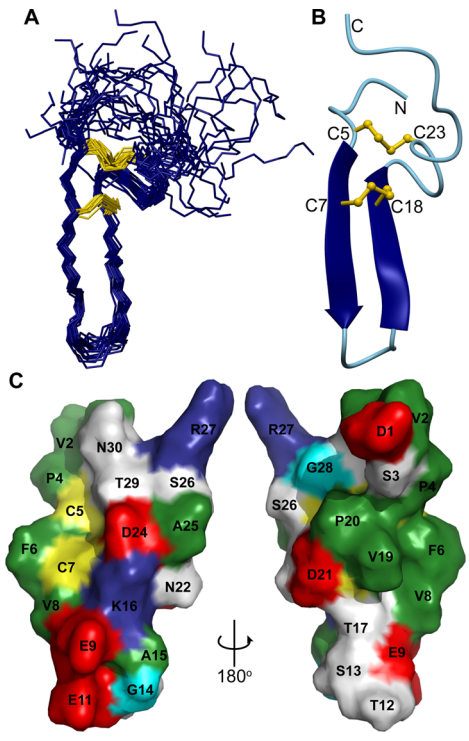

Figure 4. Three-dimensional structure of barrettide A (**1**) determined using NMR spectroscopy. (A) Superimposition of the peptide backbone from Cys5 to Cys23 of the 20 minimum energy structures of **1** with the disulfide bonds between Cys5−Cys23 and Cys7−Cys18 highlighted in yellow. (B) Ribbon representation of **1** illustrating the β-hairpin structure of the peptide, which is cross braced by the two disulfide bonds shown in ball-and-stick format (yellow). The Cys residues and the termini are labeled. (C) Surface representation of the lowest energy structure of **1**. The coloring of the surface distinguishes negatively charged (red), positively charged (blue), hydrophobic (green), polar (white), cysteine (yellow), and glycine (cyan) residues. The individual amino acids within the sequence are also labeled. The structures were determined using NMR spectroscopy, and the figures were created in MOLMOL[43] and PyMOL.

DOI: 10.1021/acs.jnatprod.5b00210
J. Nat. Prod. 2015, 78, 1886−1893

statistics for the structure ensemble are summarized in Table 1 and demonstrate that the structure is of high quality and in good agreement with both experimental data and covalent geometry. Analysis of the structure identified two antiparallel β-sheets comprising residues 6−10 and 15−19 forming a β-hairpin that is cross braced by two disulfide bonds at the base of the hairpin (Figure 4B). A tight turn occurs after the second β-strand, in which Pro20 adopts a *cis* configuration. This tight turn is presumably to allow for the ladder-like arrangement of the disulfide bonds and the difference in spacing between Cys5 and Cys7 (one residue) and Cys18 and Cys23 (four residues). As evident from the overlay of the ensemble of **1** structures, both the termini are disordered and appear to be flexible in solution, consistent with secondary Hα chemical shifts close to random coil values. The structural topology of **1**, a β-hairpin fold cross braced by two disulfide bonds in a ladder-like arrangement, is also seen in the analgesic conotoxin MrIA.[34] However, MrIA is only a 13-residue peptide, and therefore the β-hairpin is much shorter than that seen in **1**. Analysis of the surface distribution of residues reveals a clustering of hydrophobic residues consisting of Val2, Pro4, Phe6, Val8, V19, and P20 on one face of the molecule (Figure 4C). There is also a series of residues, Glu9, Glu11, Lys16, and Asp24, forming a charged region on the opposite face of the molecule from the hydrophobic surface, which suggests **1** has an amphipathic nature.

Peptide Synthesis and Oxidative Folding. In our initial attempts to synthesize **1** by manual 9*H*-fluoren-9-ylmethoxycarbonyl (Fmoc)-SPPS, peptide purity rapidly decreased after assembling the first half of the peptide sequence. Analysis of the crude peptide demonstrated poor coupling efficiencies after reaching the third cysteine (Cys18). Several factors may explain the poor efficiency: the length of the peptide chain, the presence of amino acids with β-branched side chains, and the tendency of peptides to undergo aggregation or β-sheet formation during synthesis. With the structure in hand, the poor yield is likely connected to the propensity of β-sheet formation.

In our case, we changed to microwave-assisted Fmoc-SPPS to facilitate coupling, and we also incorporated a pseudoproline dipeptide at the Glu11−Thr12 position to reduce peptide β-sheet formation during synthesis. Using this method, the peptide was synthesized on chlorotrityl chloride resin using microwave-heated coupling and deprotection steps at a temperature of 60 °C. This temperature is 10 °C lower than the one used in our standard microwave−SPPS protocol, to prevent premature cleavage of the peptide from the resin. *N*,*N*′-Diisopropylcarbodiimide (DIC) was used as the coupling agent together with the base ethyl (hydroxyimino)cyanoacetate (OxymaPure) in place of hydroxybenzotriazole (HOBT), which has been commonly used in the past.[35] The combination of DIC and OxymaPure as the coupling agent assisted by microwave heating gave a crude yield of **1** of 77.6%. The main side product was a peptide with an additional +56 Da mass that most likely resulted from an uncleaved trityl protecting group. The purified reduced **1** peptide was then oxidized under optimized folding conditions for 48 h and repurified on RP-HPLC. Folded **1** was identified by MS, and the oxidized peptide coeluted with native peptide on analytical RP-HPLC, confirming that the native disulfide connectivity was maintained in the synthetic peptide (Figure 5). A comparison of the Hα chemical shift values of synthetic and native **1** also confirmed that the correct disulfide isomer was obtained (Figure 5D).

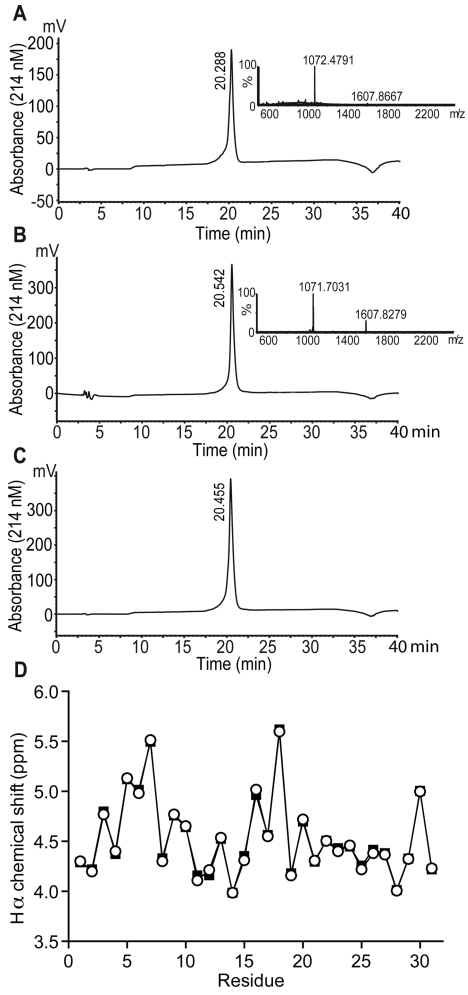

Figure 5. Comparison of native and synthetic barrettide A (**1**). (A) RP-HPLC chromatogram of synthetic **1** and mass spectrometric data (inset) confirming the expected molecular weight. (B) RP-HPLC chromatogram of native **1** including mass spectrum (inset). (C) RP-HPLC of a 1:1 mixture of synthetic and native **1** showing coelution of the two peptides. (D) Comparison of Hα chemical shifts of synthetic (solid squares) and native (open circles) of **1** in H_2O/D_2O (90:10) at 298 K.

Together, the total synthesis and NMR studies of barrettide A demonstrate unambiguous support of the sequence as determined by quantitative amino acid analysis, MS, MS-MS, and transcriptome analyses.

Biological Activity. As the barettins from *G. barretti* have previously been shown to possess antifouling properties, both **1** and **2** were tested for their effect on the settlement of barnacle larvae of *B. improvisus*. Both peptides were tested at three concentrations (0.06, 0.6, and 6 μM), and the number of settled and metamorphosed cyprids, living cyprids, and dead cyprids were counted after 4 days (Figure 6). Barretide A (**1**) significantly inhibited the settlement of larvae at both 0.6 and 6 μM (Figure 6A), whereas **2** inhibited settlement only at 6 μM (Figure 6B). These potencies of the barrettides are comparable to both barettin (EC_{50} = 0.9 μM) and 8,9-dihydrobarettin (EC_{50} = 7.9 μM)[21] but are lower than bromobenzisoxazolone barettin (EC_{50} = 15 nM)[22] and the cyclic disulfide-rich peptide cycloviolacin O2 (EC_{50} = 0.25 μM).[36] It would be interesting to assess the antifouling effect of the barrettides in combination with the barettins, as it has previously been demonstrated that a

DOI: 10.1021/acs.jnatprod.5b00210
J. Nat. Prod. 2015, 78, 1886−1893

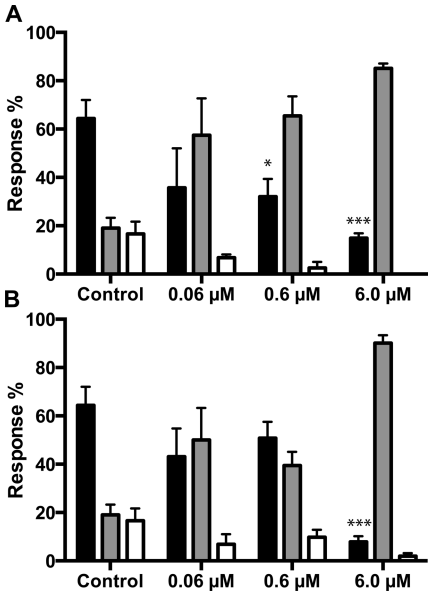

Figure 6. Effects of barrettide A and barrettide B on the settlement of cyprid larvae of *Balanus improvisus*. In the control, 64 ± 8% of barnacles settled (black bars), 19 ± 4% were alive but had not settled (gray bars), and 17 ± 5% were found dead (white bars), after 4 days of incubation in seawater. (A) Results of incubation of *B. improvisus* larvae including barrettide A in the seawater (0.06, 0.6, or 6 μM): a slight but statistically significant inhibition of settlement can be seen already at 0.6 μM, and at a concentration of 6 μM only 15 ± 2% of larvae settled. For barrettide B (B) statistically significant inhibition was demonstrated at 6 μM, at which 8 ± 2% had settled. Notably, the percentage of dead larvae decreased at higher concentrations of barrettides. Data are given as means ± SEM (n = 5, *p < 0.05, ***p < 0.001 versus control).

mixture of barettin and 8,9-dihydrobarettin acts synergistically to inhibit larval settlement.[23] Importantly, both barrettides were not toxic, as the number of dead larvae in the peptide treatments was the same as for controls after 24 h.

Many antimicrobial peptides are amphipathic in nature. However, despite having clustered regions of hydrophobic and charged residues, the barrettides showed no antibacterial activity against the Gram negative *Escherichia coli* or the Gram positive *Staphylococcus aureus* bacteria. No inhibition was detected up to a concentration of 80 μM, which is a typical cutoff value for antimicrobial peptides classifying them as inactive. In comparison, the human antimicrobial peptide LL-37 used as a control showed normal inhibitory concentrations (1−2 μM). Despite having amphipathic character, the charged residues in **1** and **2** are predominantly negative, resulting in a −4 net charge. The bacterial cell wall membrane has a high density of anionic groups and, hence, interacts better with cationic peptides, which explains why most antimicrobial peptides are positively charged.

In conclusion, we have characterized two disulfide-containing peptides, barrettides A (**1**) and B (**2**), from the cold-water marine sponge *G. barretti*. They have a unique three-dimensional structure when compared to previously described disulfide-containing peptides and expand on the diversity of this class of peptides described from marine sponges. Furthermore, we have demonstrated that the barrettides are amenable to peptide synthesis, which will facilitate future work on understanding the structure/activity relationships of this interesting family of peptides.

EXPERIMENTAL SECTION

General Experimental Procedures. RP-HPLC was performed using an Agilent 1100 binary HPLC system (Santa Clara, CA, USA) with UV detection at 215 or 230 nm for analytical and preparative HPLC, using Phenomenex (Torrance, CA, USA) Jupiter C_{18} columns [250 × 4.6 (i.d.), 5 μm, 300 Å, and 250 × 21.2 (i.d.) mm, 10 μm, 300 Å] respectively. Direct infusion MS was done on a Thermo-Finnigan LCQ Deca ion trap MS (San Jose, CA, USA) in the positive ESI mode. LC-MS and LC-MS-MS for sequencing were done in positive mode on a Waters QTof Micro (Waters, Milford, MA, USA) fed by a Waters NanoAcquity UPLC. Solution NMR data were recorded on a Bruker Avance 600 MHz spectrometer equipped with a cryoprobe. Microwave SPPS was performed on a CEM Liberty One automated microwave synthesizer (Matthews, NC, USA). Quantitative determinations of the amino acid content of the peptides were performed at the Amino Acid Analysis Centre, Department of Biochemistry and Organic Chemistry, Uppsala University. Resins, amino acids, and reagents for SPPS were obtained from Iris Biotech GmbH (Marktredwitz, Germany).

Sponge Material. Barrettides were isolated from a specimen of *Geodia barretti* Bowerbank collected in the Swedish Kosterfjord (58°52′ N, 11°5′ E) followed by homogenization and lyophilization. Dr. Paco Cárdenas identified the sample, and vouchers with the reference code MO20GB are kept at the Division of Pharmacognosy and deposited at the Museum of Evolution Herbarium, Uppsala University.

Extraction and Isolation of Peptides. A three-step extraction protocol with different ratios of CH_3CN in H_2O was employed. The first step involved incubation of the sponge in 60% CH_3CN/40% H_2O/0.1% formic acid at a concentration of 100 g/L overnight at room temperature (rt). The second step used 30% CH_3CN/70% H_2O/0.1% formic acid, and the third and last extraction step was with H_2O/0.1% formic acid. Supernatants were diluted to a final concentration of 10% CH_3CN, filtered, and then purified by RP-HPLC (first purification step) on a C_{18} column using a gradient of 0−60% B (buffer A: H_2O/0.05% TFA; buffer B: 60% CH_3CN/40% H_2O/0.045% TFA) in 60 min at a flow rate of 10 mL/min. Electrospray ionization-mass spectroscopy (ESIMS) confirmed the presence and molecular mass of peptides in each extraction step. Fractions containing peptides were subject to size-exclusion chromatography using Sephadex G-15 (second purification step) to remove low molecular weight compounds, including the barettins on a mobile phase of 60% CH_3CN/40% H_2O/0.05% TFA. Lyophilized fractions were dissolved in ∼3 mL of the mobile phase and injected into the HPLC operated at a flow rate of 0.6 mL/min. The high molecular weight fractions containing peptide(s) were repurified by RP-HPLC (third purification step) using a gradient of 25−50% buffer B in 55 min at a flow rate of 1 mL/min. Analytical RP-HPLC and ESIMS confirmed the purity and molecular masses of the peptides.

Sequence Analysis. For amino acid sequence analysis, the peptides were reduced with dithiothreitol in 0.25 M Tris-HCl containing 1 mM EDTA and 6 M guanidine-HCl (pH 8.5) for 2−3 h at 37 °C and subsequently alkylated by the addition of 50 mg of iodoacetamide. The reaction was stopped after 2−10 min by adding 0.5 M citric acid and subsequently desalted using solid-phase extraction on C_{18} columns. Samples were diluted to a final concentration of 10% CH_3CN before LC-MS-MS analysis. The reduced and alkylated peptides were cleaved by several enzymes, including trypsin, chymotrypsin, and endoproteinase Glu-C in 50 mM NH_4HCO_3 by incubating overnight at 37 °C. The sequence analysis was performed using nanospray MS-MS sequencing based on the presence of b and y-series ions (N- and C-terminal fragments). Together with the amino acid quantification data, the sequence orders for the peptides were confirmed.

NMR Spectroscopy. Samples were dissolved in 90% H_2O/10% D_2O (pH 5.15) or 100% D_2O to a final concentration of 1.2 mM and 0.62 mM for **1** and **2**, respectively. 2,2-Dimethyl-2-silapentane-5-sulfonate (DSS) was added as an internal chemical shift reference (0.0 ppm). Two-dimensional NMR spectra were recorded at 298 K, and at 283−313 K to collect temperature coefficient data, and processed by

DOI: 10.1021/acs.jnatprod.5b00210
J. Nat. Prod. 2015, 78, 1886−1893

Topspin 2.1 (Bruker). Data sets included homonuclear DQF-COSY (16 scans), TOCSY (4 scans) with a mixing time of 80 ms, and NOESY (48 scans or 64 scans) with mixing times of 100−200 ms. Spectra were recorded with a sweep width of 11.97 ppm and a resolution of 4k data points in the f2 dimension and 512 increments in the f1 dimension. In addition $^{1}H-^{15}N$ and $^{1}H-^{13}C$ HSQC data sets were recorded at natural abundance using 256 scans/128 increments and 120 scans/256 increments, respectively. For detection of slow-exchanging amides, a series of one-dimensional and TOCSY spectra were recorded after immediately dissolving the peptide in D_2O. Secondary shifts were calculated using the random coil values reported by Wishart et al.[37]

Structure Determination. Spectroscopic data were analyzed using CARA[38] and CCPNMR.[39] Spectra were assigned using the sequential assignment protocol,[29] and HSQC data were assigned based on the ^{1}H chemical shifts. NOESY spectra recorded at 298 K with a mixing time of 200 ms in both 90% H_2O/10%D_2O and 100% D_2O were used to derive interproton distance restraints. All peaks were integrated, assigned, and calibrated automatically into distance restraints using CYANA.[40] Backbone dihedral angle restraints (phi and psi) were derived from a TALOS-N analysis[31] of HN, Hα, N, Cα, and Cβ chemical shifts. The χ^1 dihedral angle conformations and stereospecific assignments of HB methylene pairs were determined from intraresidue NOE patterns derived from a 100 ms NOESY spectrum together with $^{3}J_{H\alpha-H\beta}$ coupling patterns from the DQF-COSY spectrum. Initial structures were generated using Cyana 3.0, and the final structures were calculated and refined in explicit water within CNS 1.2.[41] From the final round of calculation, 20 structures of a total of 50 were chosen to represent the solution structure of **1**, based on the lowest overall energies and good covalent geometries. Structures were analyzed using MolProbity,[42] and figures prepared using MOLMOL.[43]

Peptide Synthesis and Folding. Barettide A (**1**) was assembled on 2-Cl-trityl chloride (1.6 mmol/g, Iris Biotech) resin using a combination of manual SPPS[44] and microwave-assisted synthesis. The first Nα-Fmoc-protected amino acid, Pro31 (1.2 equiv), was coupled to the resin (312.5 mg, 1.6 mmol/g) in the presence of *N,N*-diisopropylethylamine (DIPEA; 4 equiv) and CH_2Cl_2 for (2 × 1.5 h at rt). The resin was then washed with CH_2Cl_2 (2 × 10 mL), and the coupling step repeated. The resin was successively washed with a mixture of CH_2Cl_2/MeOH/DIPEA, 17:2:1 (3 × 5 mL), CH_2Cl_2 (3 × 5 mL), dimethylformamide (DMF; 2 × 5 mL), and CH_2Cl_2 (2 × 5 mL) and then dried overnight under vacuum. The loading of the resin (0.41 mmol/g) was determined by absorbance measurement at 304 nm for the dibenzofulvene−piperidine adduct formed during a standard Fmoc test. Barettide A (**1**) was synthesized on a 0.1 mM scale with Fmoc chemistry. Solutions of 1 M DIC and 2 M OxymaPure in DMF (filtered) were prepared separately and used for *in situ* coupling. The Fmoc deprotection was carried out using 20% piperidine (20 min), and the next three C-terminal amino acids Asn30, Thr29, and Gly28 (5 equiv) were coupled using Oxymapure/DIC (10 equiv:10 equiv) at 23 °C (30 min × 2). Then the synthesis was continued until Ser13 was on the synthesizer using previously specified microwave-assisted deprotection (30 s at 60 °C, 3 min at 60 °C) and standard coupling (60 °C, 5 min) parameters.[35] Fmoc-Arg was coupled using modified conditions (25 min at 23 °C × 1, 5 min at 60 °C × 1). To facilitate assembly of the peptide chain, the psesudoproline dipeptide Fmoc-Glu(OtBu)-Thr($\Psi^{Me,Me}$ pro)-OH (5 equiv) was incorporated at positions 11 and 12 using DIC/OxymaPure (10 equiv:10 equiv) as coupling agent (30 min × 2 at 23 °C). The remaining amino acids were then coupled by microwave assistance using double-coupling cycles (5 min at 60 °C × 2). Final crude peptide was obtained in 43% yield based on the increase in resin weight.

The peptides were cleaved from resin using trifluoroacetic acid (TFA) with triisopropylsilane (TIPS) and H_2O as scavengers (9.5:2.5:2.5 TFA/TIPS/H_2O) at rt for 2 h. TFA was dried down to 0.5 mL with nitrogen, and the peptide was precipitated in ice-cold ether, filtered, and dissolved in 50% CH_3CN containing 0.05% TFA, then lyophilized. The crude peptides were purified by RP-HPLC on a C_{18} column using a gradient of 0−80% B (buffer A: H_2O/0.05% TFA; buffer B: 90% CH_3CN/10% H_2O/0.045% TFA) over 80 min. ESIMS was used to confirm the molecular mass of the synthesized peptide. Formation of the disulfide bonds was achieved by incubation of the reduced peptide (0.2 mg/mL) in a buffer consisting of 0.1 M NH_4HCO_3, 20 mM reduced glutathione, and 4 mM oxidized glutathione (pH 8.5) for 48 h at 23 °C with constant stirring. The folded peptide was purified by RP-HPLC as described previously, and its molecular weight confirmed by ESIMS. Co-injection on RP-HPLC and NMR data analysis were used to compare synthetic and isolated **1**.

Antimicrobial Testing. *E. coli* (ATCC 25922) and *S. aureus* (ATCC 29213) were grown to mid logarithmic phase in 3% tryptic soy broth at 37 °C and then washed twice by centrifugation and resuspension in 10 mM Tris buffer, pH 7.4. Serial dilutions of the two peptides (0.16 to 80 μM) were prepared in 96-well tissue culture plates to which 50 000 bacteria/well (assessed by OD_{600}) were added, giving a total volume of 100 μL. After 5 h incubation at 37 °C, 5 μL of 20% tryptic soy broth was added to each well. Plates were reincubated for 5 h or longer to generate observable microbial growth. Negative controls lacked peptide or bacteria, and the benchmark antimicrobial peptide LL-37 was used as a positive control, showing its typical 1−2 μM minimum inhibitory concentration. This MIC assay is designed to minimize interference by polyelectrolytes and amphiphilic compounds in the growth media on antimicrobial peptide activity.[45] Both peptides were tested three times (n = 3).

Antifouling Testing. The settlement propensity and mortality were used to evaluate the biological activity of **1** and **2**, as described by Sjögren et al.[21,46] Statistical analysis was performed using an unpaired Student's t-test, and differences were considered significant if $p < 0.05$.

■ ASSOCIATED CONTENT

Supporting Information

The Supporting Information is available free of charge on the ACS Publications website at DOI: 10.1021/acs.jnatprod.5b00210.

■ AUTHOR INFORMATION

Corresponding Author

*Tel: +46 18 4715031. Fax: +46 18 509101. E-mail: ulf.goransson@fkog.uu.se.

Notes

The authors declare no competing financial interest.

■ ACKNOWLEDGMENTS

B.B.C. is a holder of a University of Queensland Graduate School International Travel Award. R.J.C. is an ARC Future Fellow (FT100100476). Research at the Division of Pharmacognosy is supported by EU FP7 BlueGenics (311848; L.B.) and the Swedish Research Council (2012-5063; 2011-3403; U.G.). We thank Dr. P. Cárdenas for identification of *Geodia barretti* and support with bioinformatics; Mr. E. Jacobsson for support with bioinformatics; and Dr. A. A. Strömstedt for help with antibacterial assays.

■ REFERENCES

(1) Lazcano-Perez, F.; Roman-Gonzalez, S. A.; Sanchez-Puig, N.; Arreguin-Espinosa, R. *Protein Pept. Lett.* **2012**, *19*, 700−707.

(2) Vetter, I.; Lewis, R. J. *Curr. Top. Med. Chem.* **2012**, *12*, 1546−1552.

(3) Arnison, P. G.; Bibb, M. J.; Bierbaum, G.; Bowers, A. A.; Bugni, T. S.; Bulaj, G.; Camarero, J. A.; Campopiano, D. J.; Challis, G. L.; Clardy, J.; Cotter, P. D.; Craik, D. J.; Dawson, M.; Dittmann, E.; Donadio, S.; Dorrestein, P. C.; Entian, K. D.; Fischbach, M. A.; Garavelli, J. S.; Goransson, U.; Gruber, C. W.; Haft, D. H.; Hemscheidt, T. K.; Hertweck, C.; Hill, C.; Horswill, A. R.; Jaspars, M.; Kelly, W. L.; Klinman, J. P.; Kuipers, O. P.; Link, A. J.; Liu, W.;

DOI: 10.1021/acs.jnatprod.5b00210
J. Nat. Prod. 2015, 78, 1886−1893

Marahiel, M. A.; Mitchell, D. A.; Moll, G. N.; Moore, B. S.; Muller, R.; Nair, S. K.; Nes, I. F.; Norris, G. E.; Olivera, B. M.; Onaka, H.; Patchett, M. L.; Piel, J.; Reaney, M. J.; Rebuffat, S.; Ross, R. P.; Sahl, H. G.; Schmidt, E. W.; Selsted, M. E.; Severinov, K.; Shen, B.; Sivonen, K.; Smith, L.; Stein, T.; Sussmuth, R. D.; Tagg, J. R.; Tang, G. L.; Truman, A. W.; Vederas, J. C.; Walsh, C. T.; Walton, J. D.; Wenzel, S. C.; Willey, J. M.; van der Donk, W. A. *Nat. Prod. Rep.* **2013**, *30*, 108−160.
(4) Castaneda, O.; Harvey, A. L. *Toxicon* **2009**, *54*, 1119−1124.
(5) Shiomi, K. *Toxicon* **2009**, *54*, 1112−1118.
(6) Norton, R. S. *Toxicon* **2009**, *54*, 1075−1088.
(7) Akondi, K. B.; Muttenthaler, M.; Dutertre, S.; Kaas, Q.; Craik, D. J.; Lewis, R. J.; Alewood, P. F. *Chem. Rev.* **2014**, *114*, 5815−5847.
(8) Kaas, Q.; Westermann, J. C.; Halai, R.; Wang, C. K. L.; Craik, D. J. *Bioinformatics* **2008**, *24*, 445−446.
(9) King, G. F. *Expert Opin. Biol. Ther.* **2011**, *11*, 1469−1484.
(10) Blunt, J. W.; Copp, B. R.; Keyzers, R. A.; Munro, M. H.; Prinsep, M. R. *Nat. Prod. Rep.* **2014**, *31*, 160−258.
(11) Mehbub, M. F.; Lei, J.; Franco, C.; Zhang, W. *Mar. Drugs* **2014**, *12*, 4539−4577.
(12) Takada, K.; Hamada, T.; Hirota, H.; Nakao, Y.; Matsunaga, S.; van Soest, R. W.; Fusetani, N. *Chem. Biol.* **2006**, *13*, 569−574.
(13) Kolmar, H. *Curr. Opin. Pharmacol.* **2009**, *9*, 608−614.
(14) Olivera, B. M. *J. Biol. Chem.* **2006**, *281*, 31173−31177.
(15) Burman, R.; Gunasekera, S.; Strömstedt, A. A.; Göransson, U. *J. Nat. Prod.* **2014**, *77*, 724−736.
(16) Liu, H.; Boudreau, M. A.; Zheng, J.; Whittal, R. M.; Austin, P.; Roskelley, C. D.; Roberge, M.; Andersen, R. J.; Vederas, J. C. *J. Am. Chem. Soc.* **2010**, *132*, 1486−1487.
(17) Williams, D. E.; Austin, P.; Diaz-Marrero, A. R.; Soest, R. V.; Matainaho, T.; Roskelley, C. D.; Roberge, M.; Andersen, R. J. *Org. Lett.* **2005**, *7*, 4173−4176.
(18) Austin, P.; Heller, M.; Williams, D. E.; McIntosh, L. P.; Vogl, A. W.; Foster, L. J.; Andersen, R. J.; Roberge, M.; Roskelley, C. D. *PLoS One* **2010**, *5*, e10836.
(19) Towle, K. M.; Chaytor, J. L.; Liu, H.; Austin, P.; Roberge, M.; Roskelley, C. D.; Vederas, J. C. *Org. Biomol. Chem.* **2013**, *11*, 1476−1481.
(20) Lidgren, G.; Bohlin, L. *Tetrahedron Lett.* **1986**, *27*, 3283−3284.
(21) Sjögren, M.; Göransson, U.; Johnson, A. L.; Dahlström, M.; Andersson, R.; Bergman, J.; Jonsson, P. R.; Bohlin, L. *J. Nat. Prod.* **2004**, *67*, 368−372.
(22) Hedner, E.; Sjögren, M.; Hodzic, S.; Andersson, R.; Göransson, U.; Jonsson, P. R.; Bohlin, L. *J. Nat. Prod.* **2008**, *71*, 330−333.
(23) Sjögren, M.; Jonsson, P. R.; Dahlström, M.; Lundälv, T.; Burman, R.; Göransson, U.; Bohlin, L. *J. Nat. Prod.* **2011**, *74*, 449−454.
(24) Sjögren, M.; Dahlström, M.; Göransson, U.; Jonsson, P. R.; Bohlin, L. *Biofouling* **2004**, *20*, 291−297.
(25) Lind, K. F.; Hansen, E.; Osterud, B.; Eilertsen, K. E.; Bayer, A.; Engqvist, M.; Leszczak, K.; Jorgensen, T. O.; Andersen, J. H. *Mar. Drugs* **2013**, *11*, 2655−2666.
(26) Altschul, S. F.; Madden, T. L.; Schaffer, A. A.; Zhang, J.; Zhang, Z.; Miller, W.; Lipman, D. J. *Nucleic Acids Res.* **1997**, *25*, 3389−3402.
(27) Radax, R.; Rattei, T.; Lanzen, A.; Bayer, C.; Rapp, H. T.; Urich, T.; Schleper, C. *Environ. Microbiol.* **2012**, *14*, 1308−1324.
(28) Okonechnikov, K.; Golosova, O.; Fursov, M. *Bioinformatics* **2012**, *28*, 1166−1167.
(29) Wüthrich, K. *NMR of Proteins and Nucleic Acids*; John Wiley & Sons: New York, 1986.
(30) Wishart, D. S.; Bigam, C. G.; Yao, J.; Abildgaard, F.; Dyson, H. J.; Oldfield, E.; Markley, J. L.; Sykes, B. D. *J. Biomol. NMR* **1995**, *6*, 135−140.
(31) Shen, Y.; Delaglio, F.; Cornilescu, G.; Bax, A. *J. Biomol. NMR* **2009**, *44*, 213−223.
(32) Cornilescu, G.; Delaglio, F.; Bax, A. *J. Biomol. NMR* **1999**, *13*, 289−302.
(33) Cierpicki, T.; Otlewski, J. *J. Biomol. NMR* **2001**, *21*, 249−261.
(34) Nilsson, K. P.; Lovelace, E. S.; Caesar, C. E.; Tynngard, N.; Alewood, P. F.; Johansson, H. M.; Sharpe, I. A.; Lewis, R. J.; Daly, N. L.; Craik, D. J. *Biopolymers* **2005**, *80*, 815−823.
(35) Friligou, I.; Papadimitriou, E.; Gatos, D.; Matsoukas, J.; Tselios, T. *Amino Acids* **2011**, *40*, 1431−1440.
(36) Göransson, U.; Sjögren, M.; Svangård, E.; Claeson, P.; Bohlin, L. *J. Nat. Prod.* **2004**, *67*, 1287−1290.
(37) Wishart, D. S.; Sykes, B. D.; Richards, F. M. *Biochemistry* **1992**, *31*, 1647−1651.
(38) Keller, R. L. J. *The Computer Aided Resonance Assignment Tutorial*, 1st ed.; Cantina Verlag: Goldau, 2004.
(39) Vranken, W. F.; Boucher, W.; Stevens, T. J.; Fogh, R. H.; Pajon, A.; Llinas, M.; Ulrich, E. L.; Markley, J. L.; Ionides, J.; Laue, E. D. *Proteins: Struct., Funct., Genet.* **2005**, *59*, 687−696.
(40) Güntert, P. In *Protein NMR Techniques*; Downing, A. K., Ed.; Humana Press: 2004; Vol. *278*, Chapter 17, pp. 353−378.
(41) Brunger, A. T.; Adams, P. D.; Clore, G. M.; DeLano, W. L.; Gros, P.; Grosse-Kunstleve, R. W.; Jiang, J. S.; Kuszewski, J.; Nilges, M.; Pannu, N. S.; Read, R. J.; Rice, L. M.; Simonson, T.; Warren, G. L. *Acta Crystallogr., Sect. D: Biol. Crystallogr.* **1998**, *54*, 905−921.
(42) Chen, V. B.; Arendall, W. B., 3rd; Headd, J. J.; Keedy, D. A.; Immormino, R. M.; Kapral, G. J.; Murray, L. W.; Richardson, J. S.; Richardson, D. C. *Acta Crystallogr., Sect. D: Biol. Crystallogr.* **2010**, *66*, 12−21.
(43) Koradi, R.; Billeter, M.; Wuthrich, K. *J. Mol. Graphics* **1996**, *14*, 29−32.
(44) Merrifield, R. B. *J. Am. Chem. Soc.* **1963**, *85*, 2149−2154.
(45) Strömstedt, A. A.; Felth, J.; Bohlin, L. *Phytochem. Anal.* **2014**, *25*, 13−28.
(46) Sjögren, M.; Johnson, A. L.; Hedner, E.; Dahlström, M.; Göransson, U.; Shirani, H.; Bergman, J.; Jonsson, P. R.; Bohlin, L. *Peptides* **2006**, *27*, 2058−2064.

DOI: 10.1021/acs.jnatprod.5b00210
J. Nat. Prod. 2015, 78, 1886−1893